Synthesis and Photoluminescence of Eu-doped ZnO Nanosheets

WANG Dan-dan[1,2,3], YANG Jing-hai[3*], CAO Jian[1,2], LANG Ji-hui[3], GAO Ming[3] and LIU Xiao-yan[3]

1. Key Laboratory of Excited State Processes, Changchun Institute of Optics, Fine Mechanics and Physics, Chinese Academy of Sciences, Changchun 130033, P. R. China;

2. Graduate School of Chinese Academy of Sciences, Beijing 100049, P. R. China;

3. Institute of Condensed State Physics, Jilin Normal University, Siping 136000, P. R. China

Abstract Eu-doped ZnO nanosheets were synthesized successfully by means of the hydrothermal method. The X-ray diffraction(XRD) pattern shows that the sample is a single phase with the ZnO-like wurtzite structure. And the X-ray photoelectron spectrum suggests that there are Eu^{3+} ions in the matrix of the sample. Eu^{3+}-related red emissions resulted from energy transfer were observed for the nanosheets under UV laser excitation. The UV, green and yellow emissions were also seen in the photoluminescence spectra.

Keywords Oxide material; Chemical synthesis; Optical property

Article ID 1005-9040(2011)-02-174-03

1 Introduction

Trivalent rare-earth ions(RE^{3+}) exhibit very sharp and temperature independent RE intra-4*f* shell transition since the 4*f* shell is well shielded by the outer 5*s* and 5*p* electrons. Recently, rare-earth(RE) doped II-VI semiconductors have received significant attention due to their application in optoelectronic devices[1—3]. The use of a semiconductor host enables minority carrier injection to excite RE 4*f* shell electrons, resulting in 4*f* shell emission. In order to obtain RE-based efficient light emitter in visible and infrared regions, several studies have focused on the preparation and optical properties of the RE doped GaN[4—6]. With the same structure as that of GaN, ZnO is also a wide bandgap II-VI semiconductor(3.37 eV). It has a large exciton binding energy of 60 meV[7], which is much higher than the thermal energy at room temperature(r. t.). It is economical, environmental friendly, and exhibits high thermal and chemical stability[7—9]. These properties make it a unique host material for doping with luminescence centers and it can exhibit efficient emission even at or above r. t. ZnO-based devices are suitable UV-blue-green light emitters[10—12], but they are much less efficient for red emission. Among various RE activators, Eu-related luminescence behaves a prominent red emission around 615 nm due to intra-4*f* shell $^5D_0$-$^7F_2$ transition. So we chose Eu as the dopant and ZnO as the host to expect to achieve the red emission of Eu-doped ZnO. In the present work, we fabricated Eu-doped ZnO nanosheets *via* the hydrothermal method. The structure and photoluminescence properties of Eu-doped ZnO were studied.

2 Experimental

Eu-doped ZnO nanosheets were synthesized *via* the hydrothermal method with post-heat treatment. $Zn(NO_3)_2{\cdot}6H_2O$ was dissolved in deionized water. Eu_2O_3 powder was dissolved in dilute nitric acid to obtain a 0.01 mol/L aqueous solution of europium nitrate. The two solutions were mixed to which urea was added with a molar ratio of Zn:Eu:urea of 1:0.02:10, and the concentration of the metal ions in the solution was adjusted to 0.01 mol/L(pH *ca*. 6). After stirring, the solution was transferred into a 100 mL Teflon-lined autoclave, which was filled to nearly 80% of its capacity. Si substrate was tilted in the solution. The autoclave was kept in a dry cabinet at 120 °C for 6 h, then the solution was cooled down to r. t. There was a white film on the Si substrate that was washed them with distilled water, and then dried at 60 °C and annealed at 400 °C in air for 2 h. Herein, we named the as-grown sample EZO. The crystal structure and morphology of the samples were studied by X-ray diffraction(XRD) method, transmission electron microscopy (TEM, JEOL 2100, operated at 200 kV) and JEOL JSM-6700F field emission scanning electron microscopy(FESEM). A quantitative compositional analysis was carried out by using an X-ray photoelectron spectroscopy(XPS) in an ultra-high-vacuum chamber at a pressure lower than 1.333×10^{-7} Pa and

*Corresponding author. E-mail: jhyang1@jlnu.edu.cn

Received March 1, 2010; accepted April 12, 2010.

Supported by the National Natural Science Foundation of China(Nos.60778040, 60878039), the Program for the Development of Science and Technology of Jilin Province, China(Nos.20090140, 20090331), the Eleventh Five-Year Program for Science and Technology of Education Department of Jilin Province, China(No.20090422), the Open Project Program of National Laboratory of Superhard Materials of China(No.201004) and the Program for the Master Students' Scientific and Innovative Research of Jilin Normal University, China(No.S09010104).

peak positions were referenced to adventitious C_{1s} peak at 285.0 eV. Room temperature PL was characterized by He-Cd laser with a 325 nm excitation line. The excitation spectra were taken on a Hitachi F-4500 spectrofluorimeter equipped with a 150 W xenon lamp as the excitation source at room temperature.

3 Results and Discussion

It has been well recognized that the largest obstacle to achieve effective Eu doping is the giant mismatch between the ion radius of Eu(0.095 nm) and Zn(0.060 nm). The anion-rich environment associated with the chemical route greatly benefits the doping process by suppressing the "self-purification" mechanism[13], leading to homogeneous Eu doping. So we chose the hydrothermal method to get efficient doping of Eu ions. The decomposition of urea produced OH^- and CO_3^{2-} anions, which would form precipitates with Zn^{2+} cations, such as hydrolyzed zinc carbonate and zinc carbonate. OH^- ions were formed as a result of the reaction of NH_3 with H_2O, and CO_3^{2-} was produced by the reaction of CO_2 with OH^-:

$$CO(NH_2)_2 + H_2O = CO_2 + 2NH_3 \quad (1)$$

$$NH_3 + H_2O = NH_4^+ + OH^- \quad (2)$$

$$CO_2 + 2OH^- = CO_3^{2-} + H_2O \quad (3)$$

$$5Zn^{2+} + 2CO_3^{2-} + 6OH^- = Zn_5(CO_3)_2(OH)_6(s) \quad (4)$$

$Zn_5(CO_3)_2(OH)_6$ was pyrolysized into pure hexagonal ZnO phase after subsequent annealing(>250 °C) in air. During above chemical process, the Eu has doped into ZnO.

As the FESEM images[Fig.1(A) and (B)] show, the products appear in nanosheet. The thickness of the nanosheets is about 100 nm. They are almost perpendicular to the substrate. The nanosheets cross with each other and a layer piles on the other layer. TEM images are shown in Fig.1(C) and (D). The selected area electron diffraction(SAED) pattern in the inset suggests that the nanosheet can be indexed as the wurtzite structure with no detectable secondary phase. From the TEM image we can know that the sheets are mesoporous. The mesopores in the nanosheet might come from the Kirendall effect, in which the vacancies that balance the released molecules(H_2O, CO_2) can condense to form voids in the nanosheet[14]. In the high resolution TEM(HRTEM) image of the ZnO nanosheet[Fig.1(D)], dislocations and stacking faults are rarely observed, and the clear lattice fringes with a spacing of 0.265 nm between adjacent lattice planes correspond to the *d*-spacing of (0002) plane of ZnO.

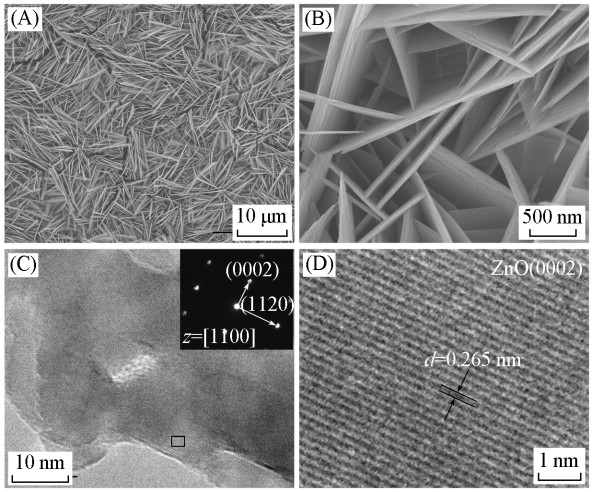

Fig.1 FESEM(A, B) and TEM(C, D) images of EZO

(D) high resolution TEM image; the inset of (C) shows the corresponding SAED pattern.

The XRD pattern of EZO shown in Fig.2 can be indexed consistently with crystalline wurtzite ZnO structure(JCPDS No. 80-0075). No impurity phase such as europium oxides was detected in the detection limit. To investigate the chemical composition and bonding states, XPS was performed on EZO. Prior to XPS measurement, the sample was cleaned by Ar ion sputtering to remove any surface contamination[15]. A typical XPS survey scan is shown in Fig.3. The survey scan confirms the presence of Zn, O, Eu and C and the absence of other impurities. Inset of Fig.3 is the core-level XPS spectrum of Eu_{3d}. The peaks at 1135.1 and 1165.5 eV correspond to $Eu_{3d5/2}$ and $Eu_{3d3/2}$, respectively[16]. Their positions indicate that the Eu ion has a +3 valence in Eu-doped ZnO nanosheets[17]. By fitting the integrated peak areas of the Zn and Eu(not shown) and using the calibrated atomic sensitivity factors, the atomic ratio of Eu to Zn was quantitatively determined to be ~1:100.

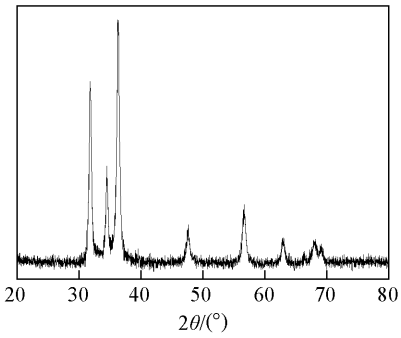

Fig.2 XRD pattern of EZO

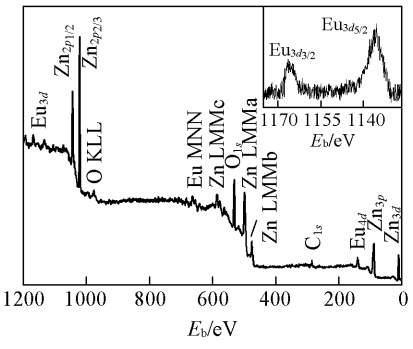

Fig.3 XPS survey spectrum of EZO

Inset is the Eu_{3d} detailed scan recorded for EZO.

Since Eu-doped ZnO often renders unique optical functionalities, we measured the PL properties of EZO. Fig.4(A) exhibits a UV emission attributed to near-band-edge(NBE) exciton recombination[18,19], a broad deep level emission band(DLE) ascribed to defects from 450 nm to 700 nm and a sharp red emission peak. Owing to the asymmetry of the broad band, we fit it into two emission bands: a green band(centered on ~520 nm) and a yellow band(centered on ~610 nm). The green band originates from oxygen vacancies located at the surface[20] and the yellow band from the oxygen interstitial not located at the surface but in the bulk[21]. Because the red emission located 612 nm is very sharp, and the full width half

maximum is 5 nm, and only rare earth ion can give such sharp emission, the red emission is attributed to the intra-4*f* transition($^5D_0$-$^7F_2$) of Eu^{3+} ions[22]. The intensity of red emission is comparable to that of intrinsic defect emission. This indicates that there is efficient energy transfer from ZnO host to Eu^{3+} ions[23]. Moreover, in the excitation spectrum[Fig.4(B)], a strong excitation peak appears at UV range that corresponds to the transition from valence band(VB) to conduction band(CB) of ZnO, which confirms the energy transfer from UV-generated delocalized electron and hole pairs in ZnO host to Eu^{3+} ions. Other excitation peaks at 392, 467 and 540 nm are likely originated from the $^7F_0$-$^5L_6$, $^7F_0$-$^5D_2$ and $^7F_1$-$^5D_1$(J=2, 1) transition of Eu^{3+} ions.

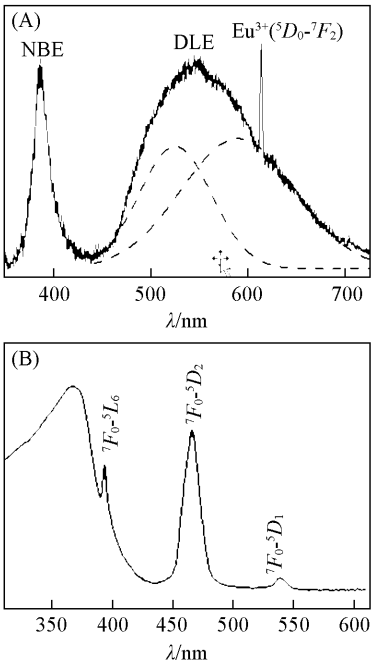

Fig.4 Room temperature PL spectrum of EZO at 325 nm excitation wavelength(A) and excitation spectrum of EZO monitored at 615 nm emission(B)

Dashed lines in (A) are fitting results.

4 Conclusions

In summary, Eu-doped ZnO nanosheets were synthesized by means of the hydrothermal method. The XRD and TEM results confirm that the production is single phase with the ZnO-like wurtzite structure. The Eu concertration is 0.99% from the caculation on the XPS result. We observed the intra-4*f* emission of Eu^{3+} due to the energy transfer from ZnO host to Eu^{3+} ions.

References

[1] Bol A. A., van Beek R., Meijerink A., *Chem. Mat.*, **2002**, *14*, 1121
[2] Wang X., Kong X. G., Shan G. Y., Yu Y., Sun Y. J., Feng L. Y., Chao K. F., Lu S. Z., Li Y. J., *J. Phys. Chem. B,* **2004**, *108*, 18408
[3] Pereira A. S., Peres M., Soares M. J., Alves E., Neves A., Monteiro T., Trindade T., *Nanotechnology*, **2006**, *17*, 834
[4] Peng H. Y., Lee C. W., Everitt H. O., Lee D. S., Steckl A. J., Zavada J. M., *Appl. Phys. Lett.*, **2005**, *86*, 51110
[5] Wang K., Martin R. W., O'Donnell K. P., Katchkanov V., Nogales E., Lorenz K., Alves E., Ruffenach S., Briot O., *Appl. Phys. Lett.*, **2005**, *87*, 112107
[6] Bodiou L., Braud A., Doualan J. L., Moncorge R., Park J. H., Munasinghe C., Steckl A. J., Lorenz K., Alves E., Daudin B., *J. Appl. Phys.*, **2009**, *105*, 043104
[7] Sun Y., Ndifor-Angwafor N. G., Riley D. J., Ashfold M. N. R., *Chem. Phys. Lett.*, **2006**, *431*, 352
[8] Xing G. Z., Yi J. B., Tao J. G., Liu T., Wong L. M., Zhang Z., Li G. P., Wang S. J., Ding J., Sum T. C., Huan C. H. A., Wu T., *Adv. Mater.*, **2008**, *20*, 3521
[9] Yang J. H., Wang D. D., Yang L. L., Zhang Y. J., Lang J. H., Fan H. G., Gao M., Wang Y. X., *J. Alloys Comp.*, **2008**, *450*, 508
[10] Özgür Ü., Alivov Y. I., Liu C., Teke A., Reshchikov M. A., Doğan S., Avrutin V., Cho S. J., Morkoc H., *J. Appl. Phys.*, **2005**, *98*, 041301
[11] Zhang X. M., Lu M. Y., Zhang Y., Chen L. J., Wang Z. L., *Adv. Mater.*, **2009**, *21*, 1
[12] Huang M. H., Mao S., Feick H., Yan H. Q., Wu Y. Y., Kind H., Weber E., Russo R., Yang P. D., *Science*, **2001**, *292*, 1897
[13] Gustavo M. D., James R. C., *Phys. Rev. Lett.*, **2006**, *96*, 226802
[14] Smigelskas A. D., Kirkendall E. O., *Trans. AIME*, **1947**, *171*, 130
[15] Xing G. Z., Yi J. B., Wang D. D., Liao L., Yu T., Shen Z. X., Huan C. H. A., Sum T. C., Ding J., Wu T., *Phys. Rev. B*, **2009**, *79*, 174406
[16] Tan X. L., Wang X. K., Geckeis H., Rabung T. H., *Environ. Sci. Technol.*, **2008**, *42*, 6532
[17] Vercaemst R., Poelman D., Fiermans L., van Meirhaeghe R. L., Laflere W. H., Cardon F., *J. Electron. Spectrosc. Relat. Phenom.*, **1995**, *74*, 45
[18] Aleksandra D. B., Leung Y. H., *Small*, **2006**, *2*, 944
[19] Wang D. D., Yang J. H., Xing G. Z., Yang L. L., Lang J. H., Gao M., Wu T., *J. Lumin.*, **2009**, *129*, 996
[20] Wang D. D., Yang J. H., Yang L. L., Zhang Y. J., Lang J. H., Gao M., *Cryst. Res. Technol.*, **2008**, *43*, 1041
[21] Li D., Leung Y. H., Djurisic A. B., Liu Z. T., Xie M. H., Shi S. L., Xu S. J., Chan W. K., *Appl. Phys. Lett.*, **2004**, *85*, 160
[22] Sadhu S., Sen T., Patra A., *Chem. Phys. Lett.*, **2007**, *440*, 121
[23] Zeng X. Y., Yuan J. L., Wang Z. Y., Zhang L., *Adv. Mater.*, **2007**, *19*, 4510